1 Investigation of the extreme wet-cold compound events changes between 2025-2049 and
2 1980-2004 using regional simulations in Greece

3 Iason Markantonis[1,2], Diamando Vlachogiannis[1], Athanasios Sfetsos[1], Ioannis Kioutsioukis[2]

4 [1]Environmental Research Laboratory, NCSR "Demokritos", 15341 Agia Paraskevi, Greece

5 [2]University of Patras, Department of Physics, University Campus 26504 Rio, Patras, Greece

6 *Correspondence to*: Iason Markantonis (jasonm@ipta.demokritos.gr)

7 **Abstract.** This paper aims to study wet-cold compound events (WCCEs) in Greece for the wet and
8 cold season November-April since these events may affect directly human activities for short or longer
9 periods as no similar research has been conducted for the country studying the past and future
10 development of these compound events. WCCEs are divided into two different daily compound events
11 (Maximum Temperature (TX) -Accumulated Precipitation (RR)) and (Minimum Temperature (TN) –
12 Accumulated Precipitation (RR)) using fixed thresholds (RR over 20 mm/day and Temperature under 0
13 °C). Observational data from the Hellenic National Meteorology Service (HNMS) and simulation data
14 from reanalysis and EURO-CORDEX models were used in the study for the historical period 1980-
15 2004. The Ensemble mean of the simulation datasets from projection models was employed for the
16 near future period (2025-2049) to study the impact of climate change on the occurrence of WCCEs
17 under the Representative Concentration Pathways (RCPs) 4.5 and 8.5 scenarios. Following data
18 processing and validation of the models, the potential changes in the distribution of WCCEs in the
19 future were investigated based on the projected and historical simulations. WCCEs determined by fixed
20 thresholds were mostly found over high altitudes with TN-RR events exhibiting a future tendency to
21 reduce particularly under the RCP 8.5 scenario and TX-RR exhibiting similar reduction of probabilities
22 for both scenarios.

23

1. Introduction

25 Extreme weather events and their linkage to climate change is a matter of high concern for many
26 scientific groups (Zanocco et al., 2018; Konisky et al., 2016; Curtis et al., 2017). In the last decade,
27 numerous scientific studies focused on the causes, frequency and impacts of extreme compound events
28 (e.g. Aghakouchak et al., 2020; Singh et al., 2021; Sadegh et al., 2018; Zscheischler et al., 2017;
29 Zscheischler and Seneviratne, 2017; Zscheischler et al., 2018). As mentioned in the Intergovernmental
30 Panel on Climate Change report on "Managing the risks of extreme events and disasters to advance
31 climate change adaptation" (IPCC SREX) (Ref 7, p. 118) compound events are defined as: (1) two or
32 more extreme events occurring simultaneously or successively, (2) combinations of extreme events
33 with underlying conditions that amplify the impact of the events, or (3) combination of events that are
34 not themselves extremes but lead to an extreme event or impact when combined (Leonard et al., 2014).

35 Recent studies have been conducted on the examination of wet-cold compound events (WCCEs) that
36 concern daily values of temperature and precipitation and the correlation of these variables
37 (Chukwudum and Nadarajah, 2022; Lhotka and Kyselý, 2021), while other studies focus on the
38 occurrence of monthly WCCEs for the historical period (Wu et al., 2019; Lemus-Canovas, 2022)
39 However, the purpose of this article is the study of fixed thresholds extreme WCCEs on daily basis in
40 Greece during the historical period (1980-2004) and how the likelihood of these events will be affected
41 by climate change, during the period 2025-2049. It has been reported that WCCEs affect the region of
42 the Mediterranean Basin, including Greece (Zhang et al., 2021). Studies using only observational data
43 at some locations (Lazoglou and Anagnostopoulou, 2019), or modeled data mostly over the broader
44 region of the Mediterranean Sea (Vogel et al., 2021; Hochman et al., 2021; de Luca et al., 2020),
45 concerning WCCEs have been conducted in the past, but not depicting analytically WCCEs in Greece,
46 a country that as a part of the Mediterranean Basin is considered a "Climate change hotspot" (Ali et al.,
47 2022). This work attempts to fill this void on the effects of climate change on WCCEs in Greece.

The examined events belong to the first category of the definition of compound events from IPCC since they refer to the simultaneous exceedance of precipitation and temperature thresholds. WCCEs may have a negative impact on people's lives by causing electricity blackouts, affecting agriculture with heavy snowfall or freezing rain and blocking transportation because of closed roads, railways or even airports (Houston et al., 2006; Llasat et al., 2014; Vajda et al., 2014). On the other hand, most of the available freshwater in the country comes from melted mountain snow during spring or summer. Finally, eco-systems, especially in mountains, may be affected by the absence of snow that climate change may cause (Demiroglu et al., 2015; Pestereva et al., 2012; Trujillo et al., 2012; García-Ruiz et al., 2011).
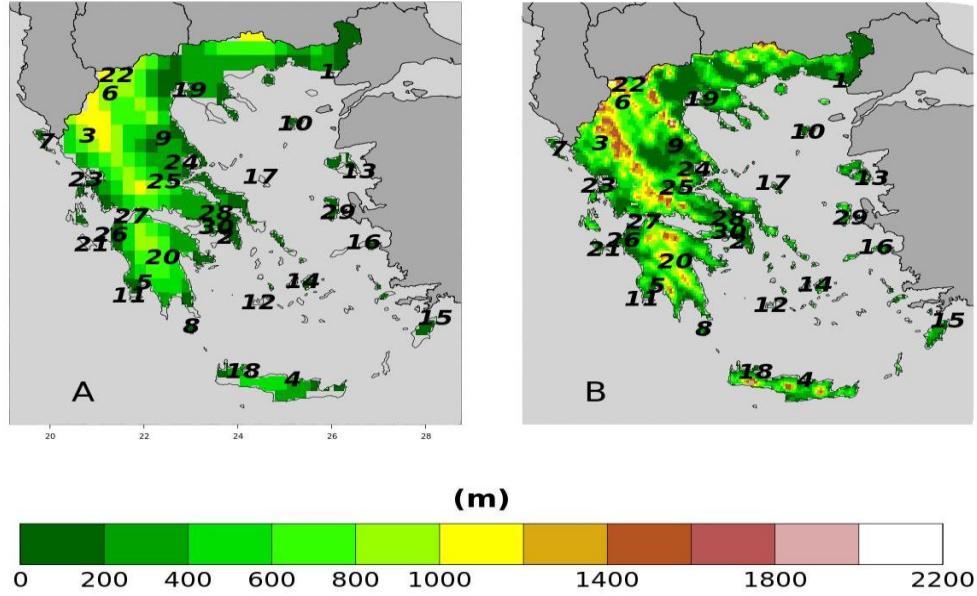
The first part of the study concerns the historical period between 1980 and 2004, because of the availability of quality-controlled daily observational data for minimum temperature (TN), maximum temperature (TX) and accumulated precipitation (RR). Hence, for that period, we use observational data from 21 Hellenic National Meteorological Service (HNMS) stations, to validate EURO-CORDEX Regional Climate Models (RCMs), provided by the Copernicus Climate Change Service and the projection model dataset produced in-house. In addition to the models, two reanalysis products are included, as the closest to "true" past climate conditions in regions with no or scarce observations (Moalafhi et al., 2016). More information about the observational and model datasets is presented in Section 2. Section 3 highlights the applied methodology while Section 4 displays WCCEs observed in stations and station cells of the models and Section 5 discusses the reanalysis and projections Ensemble mean WCCEs probabilities spatial distribution for the historical period. Section 6 details the results of the difference in WCCEs probabilities between the historical and the near future period between 2025 and 2049 for two greenhouse gas concentration scenarios, RCP 4.5 and RCP 8.5.

2. Data

In this Section, we present the datasets that provide the observational and simulation data produced by projection and reanalysis models.

2.1. HNMS observations

HNMS provides freely observational data from 21 stations for the purpose of scientific research (http://www.emy.gr/emy/el/services/paroxi-ipiresion-eleuthera-dedomena). The data have been formally evaluated by HNMS and the timeseries show no missing or distorted values. In particular, the timeseries available for the historical period 1980-2004 have a 3-hour temporal resolution and from these values, we have extracted the daily values of TN, TX and RR. Moreover, stations 22-30 which also belong to the network of HNMS stations contain observations in the period 1980-2004, although none of the stations covers all observational days in the period. The datasets of these stations were extracted by the National Centers for Environmental Information of National Oceanic and Atmospheric Administration. We selected stations that contain at least 20 years of observations. Figure 1 shows the position of the stations on the orography of ERA5 and WRF, while Table A1 of the Appendix provides details on the characteristics of the stations. We have used observational data to validate the model datasets regarding the WCCEs for the historical period.

Figure 1: Map of HNMS stations on orography of (A) ERA5 and (B) WRF-ERAinterim. The numbers correspond to those in Table A1 (Appendix).

2.2. Reanalysis models

We have used two reanalysis models due to the lack of spatially and temporally complete direct observations, to study consistently the WCCEs in Greece in the historical period. The first model is the latest available reanalysis product ERA 5 from the European Centre for Medium-Range Weather Forecasts (ECMWF) of spatial resolution ~30km x 30km (Hersbach et al., 2020). The second reanalysis model, built in the Environmental Research Laboratory (EREL) of the National Center of Scientific Research 'Demokritos' (NCSRD) WRF_ERA_I, has been produced by dynamically downscaling ERA-INTERIM using the Weather Research Forecast (WRF) model (v3.6.1) from 80km x 80km to 5km x 5km (Politi et al., 2021, 2020, 2018).

2.3. GCM / RCM models

To observe possible alterations of WCCEs occurrence probability in the future period 2025-2049 compared to the historical period, we employed data from RCM simulations driven by GCMs. In this regard, we obtained data from 5 models included in the EURO-CORDEX initiative provided by the Copernicus Program. All chosen EURO-CORDEX models with available daily data for both RCP scenarios were selected because they have the finest spatial resolution of 0.11° x 0.11°, and have also been tested in Cardoso et al, (2019). Information on the regional and parent models and their acronyms used herewith is given in Table 1. In addition to the EURO-CORDEX model data, we have used dynamically downscaled data from the EC-EARTH GCM to a high spatial resolution of 5km x 5km for the area of Greece using the WRF model (Politi et al., 2020, 2022).

Institution	Reference	Regional Model	Forcing model	Acronym	Resolution (°)
Météo-France / Centre National de Recherches Météorologiques	(Spiridonov et al., n.d.)	ALADIN63	CNRM-CERFACS-CNRM-CM5	CNRM	0.11
Koninklijk Nederlands Meteorologisch Instituut	(van Meijgaard et al., 2008)	KNMI-RACMO22E	ICHEC-EC-EARTH	KNMI	0.11

Climate Limited-Area Modelling Community	(Rockel et al., 2008)	CLMcom-CLM-CCLM4-8-17	MOHC-HadGEM2-ES	CLMcom	0.11
Swedish Meteorological and Hydrological Institute	(Samuelsson et al., 2016)	SMHI-RCA4	MPI-M-MPI-ESM-LR	SMHI	0.11
Danish Meteorological Institute	(Christensen, 2006)	DMI-HIRHAM5	NCC-NorESM1-M	DMI	0.11
EREL (NCSRD)	(Politi et al. 2020, 2022)	ARW-WRF	EC-EARTH	WRF_EC	0.05

Table 1: EURO-CORDEX and EREL-NCSRD simulation models information.

3. Methodology

The first step in this study is the validation of the projection and reanalysis models against observations. Moreover, the ensemble of the 6 projection models is also exhibited. We choose as the Ensemble resolution of the CORDEX models since 5 of them share the same spatial resolution. The only model in need of regridding is WRF_EC. We follow the nearest neighbor method to upscale WRF_EC from 5 km to 11 km. In addition, we use box-plots to depict the ability of the models to simulate observational data WCCEs probabilities for the historical period at the cells that include meteorological stations. The box plots consist of the colored box, where in the band near the middle of the box is the median, bottom and top of each color box are the 25th (Q1) and 75th (Q3) percentiles (BL) percentile. The lower limit of the whisker (LLW) is calculated by LW= Q1-1.5*BL and the upper limit (ULW) by UW= Q3+1.5*BL. The length of the whiskers (WL) is calculated as the difference between ULW and LLW. Any value out of this range is marked by a black point in the plot. The validation is conducted after the elevation bias correction of temperature at the cells of the models containing the stations. The cells of the stations are found using the nearest neighbor approach and the temperature bias correction temperature is the following:

$$T_s = T_m + 0.006*(H_m-H_s) \tag{1}$$

In equation (1), T_s is the temperature of the cell after the elevation bias correction, T_m is the temperature provided by the model, H_m is the cell elevation and H_s is the elevation of the HNMS station.

3.1. Compound event selection

According to HNMS, the meteorological year can be split into two climate periods (http://emy.gr/emy/el/climatology/climatology). The cold and wet period extends on average from mid-October to the end of March, and the warm-dry period occurs during the rest of the year. Since the study is focused on the extreme WCCEs, we examine the period between November and April, since according to the HNMS observations, April exhibits lower temperatures than October and more rainy days. Moreover, it is not uncommon for the northern parts of Greece, especially mountainous areas, to be affected by snowfalls during April. This leads to the creation of a timeseries of 4532 daily values for the historical period and 4531 for the future period. CLMcom considers that each month is consisted of 30 days, thus leading to 4500 values for each period. Also, DMI considers that a calendar year has 365 days, thus each period examined has 4525 values.

The WCCEs, which are examined on daily basis, are divided into two types of synchronous events, TX-RR and TN-RR and studied using the fixed threshold approach (Table 2). This approach considers the fixed threshold of 20 mm/day for RR and 0 °C for TN and TX for all stations or grid points, as recommended by the Commission for Climatology (CCl), the World Climate Research Programme

4

146 (WCRP) of the Climate Variability and Predictability Component (CLIVAR) project and the Expert
147 Team for Climate Change Detection and Indices (ETCCDI). TN equal to or under 0 °C indicates Frost
148 Days (FD), while TX equal to or under 0 °C indicates Iced Days (ID) (Fonseca et al., 2016). The
149 thresholds examined have been proposed in various works for studying extreme events (Raziei et al.,
150 2014; Tošić and Unkašević, 2013; Anagnostopoulou and Tolika, 2012; Pongrácz et al., 2009;
151 Kundzewicz et al., 2006; Moberg et al., 2006).

THRESHOLDS	RR	TN	TX	WCCE	
FIXED	>= 20 mm/day (RR20)	<= 0 °C (FD)	<= 0 °C (ID)	1. 2.	(RR20-FD) (RR20-ID)

152

Table 2: Univariate thresholds and the compound events examined in the study.

3.2. WCCEs probability calculation

155 The WCCEs probabilities are calculated by applying two different methods. The first is the empirical
156 approach counting the events from the timeseries and dividing by the total number of days to find the
157 percentage (%) of the occurrence probability. For the second method, we use the copula approach for
158 the HNMS observations and model comparison and to map the differences between the two methods
159 for the reanalysis and projection of model data. Compared to copula, an empirical method has a higher
160 uncertainty when calculating the probability of extreme events (Hao et al., 2018; Tavakol et al., 2020;
161 Zscheischler and Seneviratne, 2017). The purpose of using two different methods is to investigate
162 whether the copula method underestimates or overestimates the WCCEs.

163 The best fitting copula selection for each timeseries is examined using the R programming language
164 function BiCopSelect as suggested in (Zhou et al., 2019) package VineCopula (Schepsmeier et al.,
165 2013). The appropriate bivariate copula for each dataset is chosen by the function, from a multitude of
166 40 different copula families using the Akaike Information Criterion (AIC) (Akaike, 1974) and
167 Bayesian Information Criterion (BIC)   , and the copula chosen for each station and model dataset is
168 shown in Appendix B (Tables B1 and B2). Copulas are used in plenty of studies that investigate the
169 dependence between two different climate variables and the joint probability of compound events
170 (Tavakol et al., 2020; Dzupire et al., 2020; Pandey et al., 2018; Cong and Brady, 2012; Abraj and
171 Hewaarachchi, 2021).

172 As mentioned in Nelsen, (2007), a bivariate copula is a bivariate distribution function where margins
173 are uniform on the unit interval [0, 1]. A bivariate copula is a map $C:[0,1]^2 \rightarrow [0,1]$ with $C(u,1)=u$ and
174 $C(1,v)=v$. Let X and Y be random variables with a joint distribution function $F(x,y)=Pr(X \leq x, Y \leq y)$ and
175 continuous marginal distribution functions $F_1(x)=Pr(X \leq x)$ and $F_2(y)=Pr(Y \leq y)$, respectively. By Sklar's
176 theorem (Sklar, 1959), one obtains a unique representation as follows:

177 $F(x,y) = C\{F_1(x),F_2(y)\}$ (2)

178 For the two random variables of X (e.g., precipitation) and Y (e.g., temperature) with cumulative
179 distribution functions (CDFs) $F_1(x)=Pr(X>=x)$ and $F_2(y)=Pr(Y<=y)$, the bivariate joint distribution
180 function or copula (C) can be written as:

181 $F(x,y) =Pr(X>=x,Y<=y) = C(u,v)$ (3)

4. WCCEs assessment in HNMS stations

183 In this section, the models are validated against observations both for the empirical and the copula
184 method. WCCEs probabilities for each station and model are presented in the supplementary material.
185 BIAS and RMSE along with the Critical Success Index (CSI) are used for the validation. CSI is
186 calculated as CSI=A/(A+B+C). A, B and C symbolize elements from the contingency table (Table 2)
187 that occur from comparing zero and non-zero probabilities in stations with the corresponding model
188 cells. Also, the total number of events calculated for both methods from observational data is presented
189 for each station.

"EVENT"=POSITIVE PROBABILITY		OBSERVATION EVENT	
		YES	NO
MODEL	YES	**A**	**B**
EVENT	NO	**C**	**D**

Table 2: Contingency table where "A" is the number of event forecasts that correspond to event observations or the number of hits. Entry "B" is the number of event forecasts that do not correspond to observed events or the number of false alarms. Entry "C" is the number of no-event forecasts corresponding to observed events or the number of misses. Entry "D" is the number of no-event forecasts corresponding to no events observed or the number of correct rejections.

4.1. RR20FD

Probability values for each station are presented in Supplementary (Tables S1-S4) as well as the contingency tables (Tables S7-S10) from which CSI is calculated. ERA5 and WRF_ERA_I are reanalysis products and exhibited for comparison reasons. The copulas selected by Bicopselect for each observational and modeled timeseries are also presented in Supplementary (Tables S5-S6).
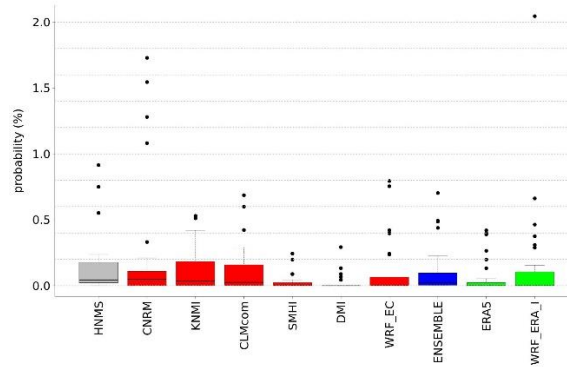

Figure 2: Box-plot presenting RR20FD empirical method probabilities for observations and models.

	HNMS	CNRM	KNMI	CLMcom	SMHI	DMI	WRF_EC	ENSEMBLE	ERA5	WRF_ERA_I
MEAN	**0.1382**	0.2361	0.1168	0.1116	0.0267	0.0208	0.1143	**0.1044**	0.0625	0.1535
SD	**0.2211**	0.4821	0.1590	0.1781	0.0581	0.0600	0.2216	**0.1813**	0.1311	0.3935
BIAS		-0.0979	0.0214	0.0266	0.1115	0.1174	0.0239	**0.0338**	0.0756	-0.0154
RMSE		0.3234	0.1298	0.0922	0.2003	0.2148	0.1222	**0.0975**	0.1536	0.2319
COR		0.8583	0.8138	0.9211	0.9194	0.7177	0.8484	**0.9118**	0.8210	0.8523
CSI		0.6071	0.6667	0.6296	0.3214	0.1667	0.3793	**0.7692**	0.2667	0.4483

Table 3: Table exhibiting mean (MEAN) station RR20FD empirical probabilities (%) for observations and models, standard deviation (SD), bias (BIAS), rmse (RMSE), Pearson correlation (COR) and CSI of models against observations.
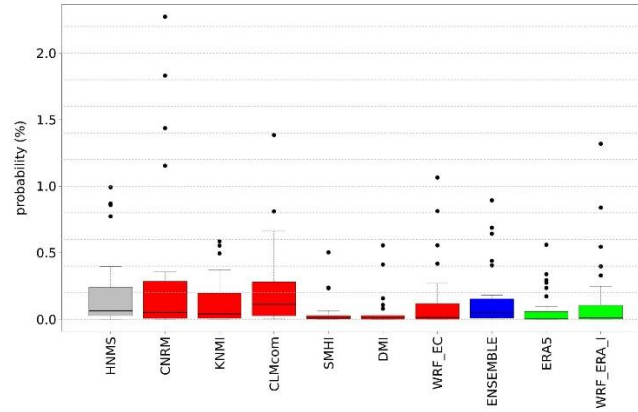
208

Figure 3: Box-plot presenting RR20FD copula method probabilities for observations and models.

	HNMS	CNRM	KNMI	CLMcom	SMHI	DMI	WRF_EC	ENSEMBLE	ERA5	WRF_ERA_I
MEAN	**0.2016**	0.2974	0.1291	0.2129	0.0448	0.0528	0.1338	**0.1451**	0.0699	0.1455
SD	**0.2864**	0.5802	0.1715	0.3031	0.1042	0.1237	0.2580	**0.2310**	0.1368	0.2939
BIAS		-0.0959	0.0725	-0.0113	0.1568	0.1488	0.0678	**0.0565**	0.1317	0.0561
RMSE		0.3334	0.1720	0.2264	0.2646	0.2530	0.1458	**0.1139**	0.2165	0.1788
COR		0.9422	0.8782	0.6968	0.7688	0.7620	0.8888	**0.9467**	0.8955	0.8233
CSI		0.9259	0.9629	1	0.9643	0.7333	0.8276	**1**	0.6333	0.7931

210 Table 4: Table exhibiting mean (MEAN) RR20FD copula station probabilities (%) for
211 observations and models, standard deviation (SD), bias (BIAS), rmse (RMSE), Pearson
212 correlation (COR) and CSI of models against observations.

213

214   **4.2. RR20ID**

215 RR20ID events yield, as expected, lower probabilities than RR20FD events as observed in Figures 4
216 and 5. Most observations and models yield zero probabilities, hence validation of models for these
217 events is limited. The empirical method exhibits eight stations with non-zero probabilities in the
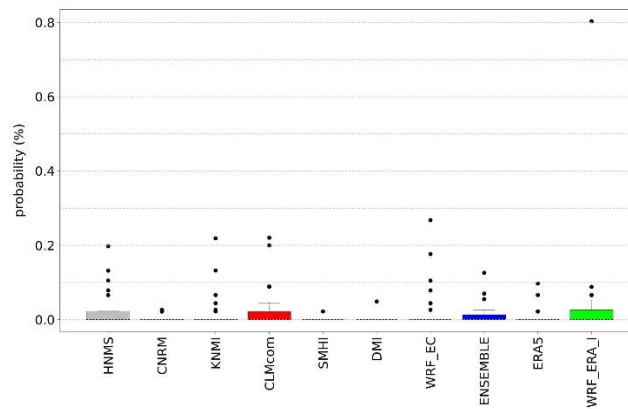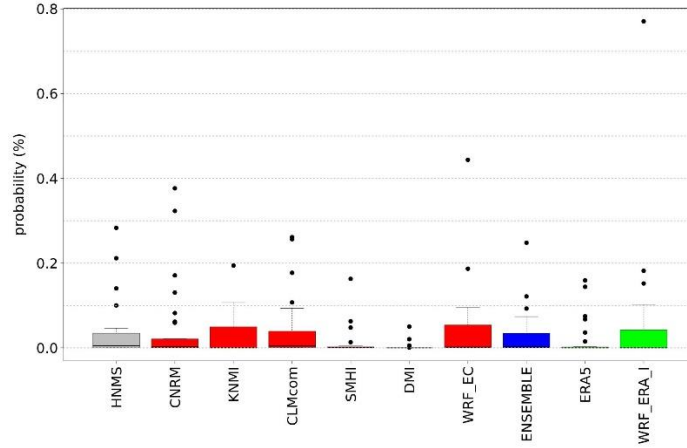218 historical period (Supplementary).

219

220

221 Figure 4: Box-plot presenting RR20ID empirical method probabilities for observations and
222 models.

	HNMS	CNRM	KNMI	CLMcom	SMHI	DMI	WRF_EC	ENSEMBLE	ERA5	WRF_ERA_I

7

	HNMS	CNRM	KNMI	CLMcom	SMHI	DMI	WRF_EC	ENSEMBLE	ERA5	WRF_ERA_I
MEAN	**0.0331**	0.0430	0.0240	0.0397	0.0104	0.0029	0.0388	**0.0265**	0.0167	0.0493
SD	**0.0669**	0.0933	0.0440	0.0725	0.0320	0.0098	0.0876	**0.0524**	0.0413	0.1441
BIAS		-0.0099	0.0091	-0.0065	0.0228	0.0303	-0.0057	**0.0067**	0.0164	-0.0161
RMSE		0.0568	0.0466	0.0556	0.0522	0.0682	0.0636	**0.0419**	0.0438	0.1084
COR		0.7961	0.7212	0.6780	0.7506	0.5380	0.6829	**0.7776**	0.8101	0.6928
CSI		0.1071	0.2000	0.1923	0.0333	0.0333	0.1481	**0.2400**	0.1034	0.1538

Table 5: Table exhibiting mean (MEAN) RR20ID empirical probabilities station probabilities (%) for observations and models, standard deviation (SD), bias (BIAS), rmse (RMSE), Pearson correlation (COR) and CSI of models against observations.

Figure 5: Box-plot presenting RR20ID copula method probabilities for observations and models.

	HNMS	*CNRM*	*KNMI*	*CLMcom*	*SMHI*	*DMI*	*WRF_EC*	*ENSEMBLE*	*ERA5*	*WRF_ERA_I*
MEAN	**0.0282**	0.0378	0.0169	0.0344	0.0066	0.0017	0.0249	**0.0204**	0.0138	0.0274
SD	**0.0663**	0.0811	0.0303	0.0676	0.0166	0.0046	0.0473	**0.0364**	0.0377	0.0524
BIAS		-0.0097	0.0112	-0.0062	0.0215	0.0264	0.0032	**0.0078**	0.0144	0.0008
RMSE		0.0532	0.0493	0.0598	0.0565	0.0691	0.0489	**0.0443**	0.0420	0.0339
COR		0.7534	0.7228	0.5861	0.8202	0.2291	0.6594	**0.7712**	0.8370	0.8540
CSI		0.5000	0.4333	0.8095	0.5357	0.2667	0.5000	**0.8095**	0.2667	0.4286

Table 6: Table exhibiting mean (MEAN) RR20ID copula probabilities station probabilities (%) for observations and models, standard deviation (SD), bias (BIAS), rmse (RMSE), Pearson correlation (COR) and CSI of models against observations.

4.3. Observations-models comparison conclusions

The events examined are rare among the available stations for the historical period. Copulas considering the dependence between the variables yield greater probabilities than the empirical method. More stations with non-zero probabilities enable more accurate validation of the models. To minimize uncertainties, smooth extreme underestimations or overestimations of WCCE probabilities that each model yields, and because ENSEMBLE shows better consistency among the projection models' statistical indices, we use it for further analysis in the study.
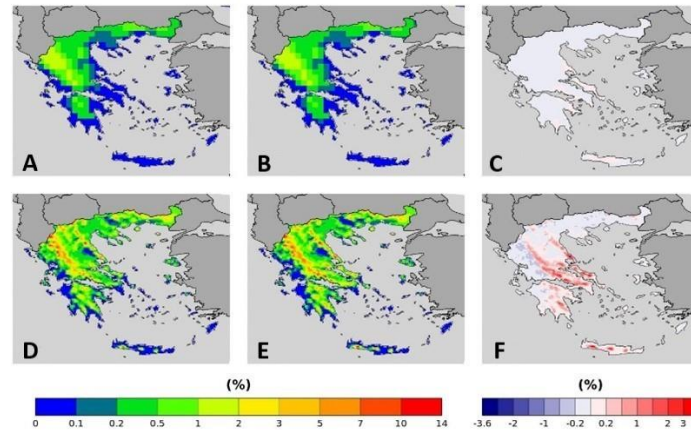
5. Historical period models WCCEs on maps

In this section, WCCEs spatial distribution probabilities are compared between empirical and copula methods. This procedure is conducted separately for the two reanalysis products and the Ensemble mean of the projection models.
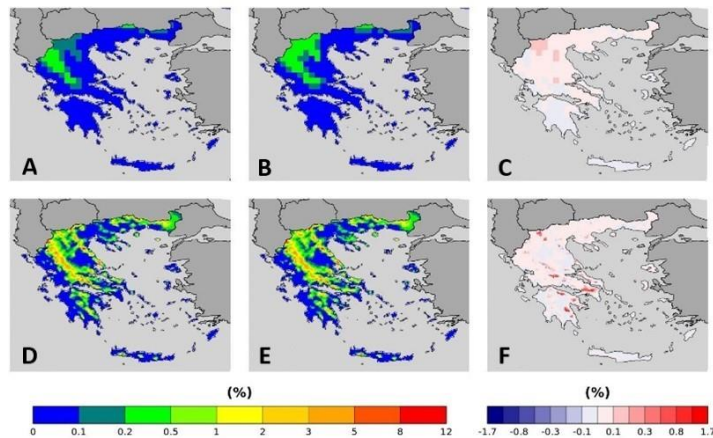
5.1. Reanalysis

ERA5 and WRF_ERA_I WCCEs spatial distribution probabilities in Greece are displayed in this section. We display both reanalysis products, although ERA5 is the most recently developed reanalysis product, we exhibit also WRF_ERA_I since its much finer spatial resolution is more appropriate for the complex topography of Greece with many mountains and islands.

Figure 6: RR20FD probabilities for (A, B, C) ERA5 and (D, E, F) WRF_ERA_I produced by (A, D) Empirical and (B, E) Copula and © = (B) –(A) and (F)=(E)-(D).
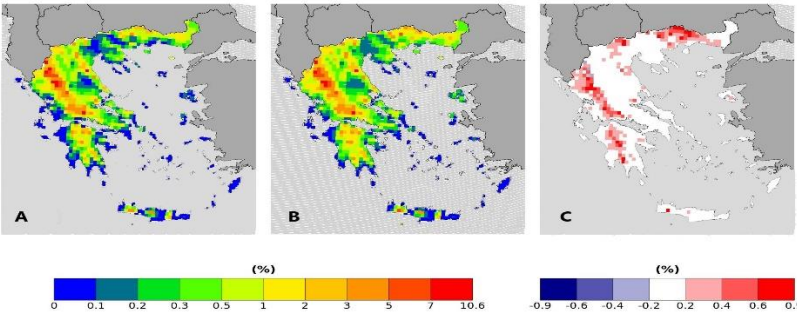

Figure 7: RR20ID probabilities for (A, B, C) ERA5 and (D, E, F) WRF_ERA_I produced by (A, D) Empirical and (B. E) Copula a©(C) = (B)–(A) and (F) = (E)-(D).

Both reanalysis products yield greater WCCEs probabilities in the Pindus mountains, although due to its finer spatial resolution, WRF_ERA_I display high probabilities at other mountainous regions located in Crete, Peloponnese, Evia Island and others. Also, in both WCCEs copula method yields higher probabilities, especially for WRF_ERA_I and the RR20FD case. Moreover, WRF_ERA_I displays a greater range than ERA5 with RR20FD probabilities reaching 14% and RR20ID 12% compared to 6% and 2% of ERA5 respectively.

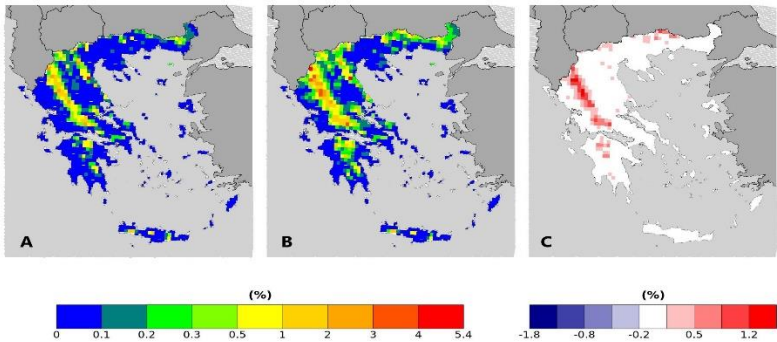## 5.2. Projections Ensemble

Figures 8 and 9yield that the Ensemble mean displays similar to the WRF_ERA_I spatial distributions of WCCEs. RR20FD and RR20ID probabilities reach 10.8% and 5.4% respectively. The copula method yields higher probabilities for both methods in mountainous regions with greater differences

displayed for RR20ID events in the Pindos mountain range and RR20FD exhibiting greater spatial distribution in differences between the two methods.

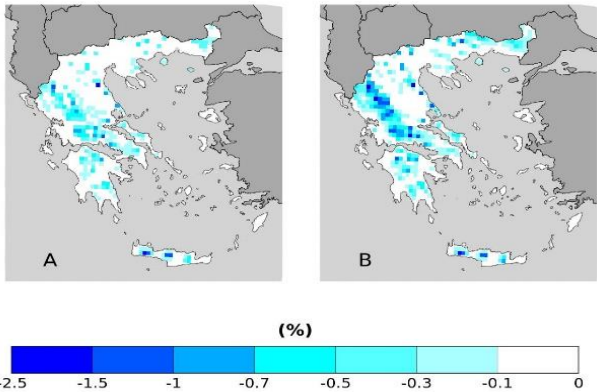**Figure 8: RR20FD Ensemble probabilities for (A) Empirical and (B) Copula method. (C)=(B)-(A).**

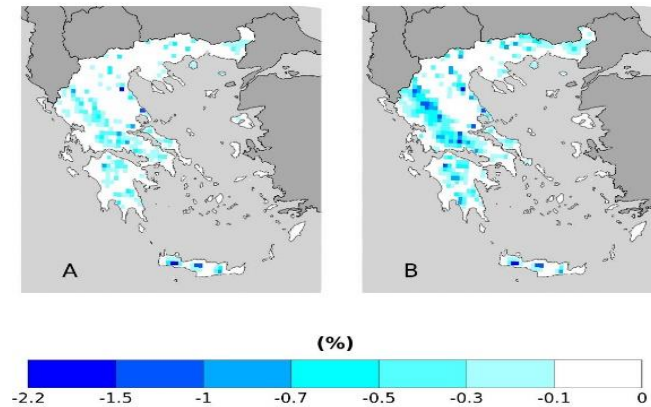**Figure 9: RR20ID Ensemble probabilities for (A) Empirical and (B) Copula method. (C)=(B)-(A).**

6.   Past-Future Ensemble differences

This section displays the differences of the Ensemble mean WCCEs probabilities, calculated for the empirical and the copula method, compared to the past probabilities presented in the previous section. The differences mapped are statistically significant at a 95% level using the Student's t-test (Goulden, 1939) comparing 25 annual values of the timeseries.

6.1. RR20FD

Figure 10: RR20FD empirical method probability differences of future-past periods for (A)
RCP4.5 and (B) RCP8.5 scenarios.

Figure 11: RR20FD copula method probability differences of future-past periods for (A) RCP4.5
and (B) RCP8.5 scenarios.

	Empirical RCP4.5	*Empirical RCP8.5*	*Copula RCP4.5*	*Copula RCP8.5*
0<=Nc>-0.1	34	31	64	57
-0.1<=Nc>-0.3	112	154	112	131
-0.3<=Nc>-0.5	63	65	53	81
-0.5<=Nc>-0.7	31	48	16	47
-0.7<=Nc>-1	12	34	6	24
-1<=Nc>-1.5	5	18	3	11
Nc<=-1.5	2	5	3	4
MAX D	**-1.8063 %**	**-2.4988 %**	**-1.9500 %**	**-2.1392 %**

Table 7: ENSEMBLE Number of cells (Nc) in each category of probability difference (%) for
RR20FD for empirical and copula method. MAX D denotes the maximum negative difference
between future and past periods. Nv concerns only cells with statistically significant difference.

From the results displayed in Figures 10 and 11 and in Table 7 RCP4.5 and RCP8.5 scenarios for the
probabilities of the RR20FD events, we observe that in all cases future scenarios yield only negative
values, meaning the reduction of RR20FD events in the 2025-2049 period compared to 1980-2004
period in all mountainous regions of Greece. RCP8.5 yields a greater reduction of RR20FD
probabilities than the RCP4.5 scenario both in spatial distribution and extreme values. The empirical
method exhibits a greater reduction for the RCP8.5 scenario, although for the RCP4.5 scenario both
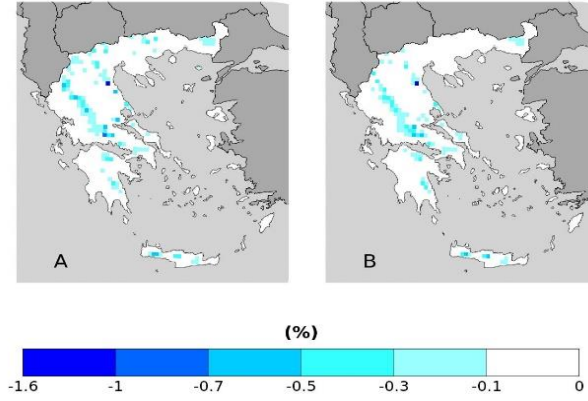methods yield similar results.

6.2. RR20ID

(%)

-1.6 -1 -0.7 -0.5 -0.3 -0.1 0

297

Figure 12: RR20ID empirical method probability differences of future-past periods for (A) RCP4.5 and (B) RCP8.5 scenarios.
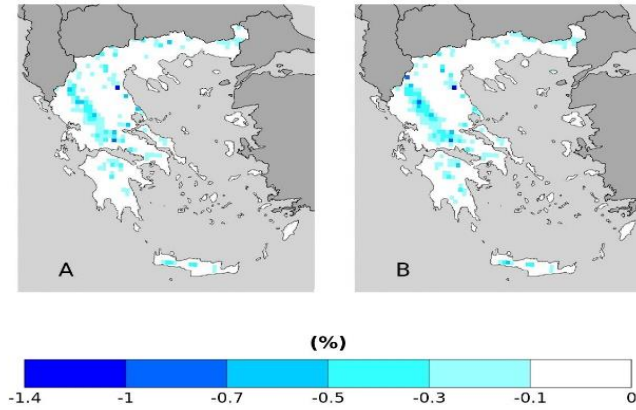

(%)

-1.4 -1 -0.7 -0.5 -0.3 -0.1 0

300

Figure 13: RR20ID copula method probability differences of future-past periods for (A) RCP4.5 and (B) RCP8.5 scenarios.

	Empirical RCP4.5	*Empirical RCP8.5*	*Copula RCP4.5*	*Copula RCP8.5*
0<=Nc>-0.1	193	229	166	210
-0.1<=Nc>-0.3	81	71	96	109
-0.3<=Nc>-0.5	23	20	33	37
-0.5<=Nc>-0.7	9	5	9	7
-0.7<=Nc>-1	1	0	1	3
Nc<=-1	1	1	1	1
MAX D	-1.5536	-1.0593	-1.3425	-1.1362

Table 8: ENSEMBLE Number of cells (Nc) in each category of probability difference (%) for RR20ID for empirical and copula method. MAX D denotes the maximum negative difference between future and past periods. Nv concerns only cells with statistically significant difference.

Similarly, to RR20FD, RR20ID events probabilities yield only zero or negative differences compared to the past for both scenarios. Empirical and copula methods yield similar results in distribution and extreme values. For both methods, the RCP4.5 scenario tends to higher reduction of RR20ID probabilities than RCP8.5, as observed in Table 8.

The results for both scenarios and events show that independently from the choice of scenario, the probabilities of the events are expected to reduce almost equally in the near future (2025-2049) compared to the past period (1980-2004).

12

7. Discussion and Conclusions

This work presents for the first time to our knowledge an extensive study of wet-cold compound events in Greece for the historical and future periods of 1980-2004 and 2025-2049, respectively. Models' data from the EUROCORDEX initiative of 0.11° resolution and reanalysis data (ERA5 and ERA-Interim dynamically downscaled to 5km^2) were used and validated for the determined WCCEs against the formally available observational datasets by HNMS for the country. The number of events and their probabilities of occurrence were determined by applying a fixed thresholds approach. Then, the bivariate validation of the models' datasets against observations was performed for the determined bivariate thresholds. The probabilities of WCCEs were computed using the empirical method and the best-fitted copula for the bivariate timeseries for observational data, reanalysis, projection models and the Ensemble of the projection models. Copulas yield higher extreme events probabilities for most of the cases considering the dependence between temperature and precipitation.

Although uncertainties may rise on the impact of WCCEs on mountainous areas due to the absence of observations on altitudes higher than 1000 meters, we trust the results yielded by the Ensemble. Besides the satisfying results from the bivariate validation, this trust is enhanced by the fact that winter period systems affect large areas crossing the country from north to south or from west to east (Cartalis et al., 2010) and therefore recorded by available stations. Also, in the cold period of the year, convective precipitation forced by orography is limited hence the doubt that the models do not simulate extreme rainfall in winter is reduced. Moreover, the use of the Ensemble mean of the models reduces the uncertainties in models' ability to simulate the probability of the occurrence of extreme events. The reduction of RR20-FD and RR20-ID WCCEs on mountains that the Ensemble of projection models predict in the future, might contribute to less heavy snowfall events and possibly less accumulated snow depth. If such a scenario will be verified, Greece faces the threat of losing the main sources of fresh water that come from melted mountain snow during spring or early summer in the near future period. The rise of temperature due to global warming is the main factor for the reduction of WCCEs (Supplementary Figures S5-S7), while also possible changes in patterns of teleconnections may affect winter conditions in Greek mountains, similar to NAO (North Atlantic Oscillation) pattern affecting Pindos mountains (López-Moreno et al., 2011) or the positive phase of EAWR (East Atlantic-Western Russia) pattern that leads to cold air advection from the north towards the southern part of Europe and the eastern Mediterranean region (Ionita, 2014). Still, understanding extreme events on complex terrains demands greater effort from the scientific community to enable solid predictions on the impact of climate change on the occurrence of these events.

Acknowledgments

References

Abdi, H.: The Kendall Rank Correlation Coefficient, 2007.

Abraj, M. A. M. and Hewaarachchi, A. P.: Joint return period estimation of daily maximum and minimum temperatures using copula method, 66, 175–190, https://doi.org/10.17654/AS066020175, 2021.

Aghakouchak, A., Chiang, F., Huning, L. S., Love, C. A., Mallakpour, I., Mazdiyasni, O., Moftakhari, H., Papalexiou, S. M., Ragno, E., and Sadegh, M.: Climate Extremes and Compound Hazards in a Warming World, 48, 519–548, https://doi.org/10.1146/ANNUREV-EARTH-071719-055228, 2020.

Akaike, H.: A New Look at the Statistical Model Identification, 19, 716–723, https://doi.org/10.1109/TAC.1974.1100705, 1974.

Ali, E., Cramer, W., Carnicer, J., Georgopoulou, E., Hilmi, N. J. M., le Cozannet, G., Lionello, P., Pörtner, H.-O., Roberts, D. C., Tignor, M., Poloczanska, E. S., Mintenbeck, K., Alegría, A., Craig, M.,

Langsdorf, S., Löschke, S., Möller, V., Okem, A., and Rama, B.: SPM 2233 CCP4 Mediterranean Region to the Sixth Assessment Report of the Intergovernmental Panel on Climate Change [, 2233–2272, https://doi.org/10.1017/9781009325844.021, n.d.

Anagnostopoulou, C. and Tolika, K.: Extreme precipitation in Europe: Statistical threshold selection based on climatological criteria, 107, 479–489, https://doi.org/10.1007/S00704-011-0487-8/TABLES/2, 2012.

Balkema, A. A. and Haan, L. de: Residual Life Time at Great Age, 2, 792–804, https://doi.org/10.1214/AOP/1176996548, 1974.

Cartalis, C., Chrysoulakis, N., Feidas, H., and Pitsitakis, N.: International Journal of Remote Sensing Categorization of cold period weather types in Greece on the basis of the photointerpretation of NOAA/AVHRR imagery Categorization of cold period weather types in Greece on the basis of the photointerpretation of NOAA/AVHRR imagery, https://doi.org/10.1080/01431160310001632684, 2010.

Cardoso, R. M., Soares, P. M. M., Lima, D. C. A., and Miranda, P. M. A.: Mean and extreme temperatures in a warming climate: EURO CORDEX and WRF regional climate high-resolution projections for Portugal, 52, 129–157, https://doi.org/10.1007/S00382-018-4124-4/FIGURES/8, 2019.

Christensen, O. B.: Regional climate change in Denmark according to a global 2-degree-warming scenario, 2006.

Chukwudum, Q. C. and Nadarajah, S.: Bivariate Extreme Value Analysis of Rainfall and Temperature in Nigeria, Environmental Modeling and Assessment, 27, 343–362, https://doi.org/10.1007/S10666-021-09781-7/TABLES/13, 2022.

Coles, S.: An Introduction to Statistical Modeling of Extreme Values, https://doi.org/10.1007/978-1-4471-3675-0, 2001.

Cong, R. G. and Brady, M.: The interdependence between rainfall and temperature: Copula analyses, 2012, https://doi.org/10.1100/2012/405675, 2012.

Curtis, S., Fair, A., Wistow, J., Val, D. v., and Oven, K.: Impact of extreme weather events and climate change for health and social care systems, 16, 23–32, https://doi.org/10.1186/S12940-017-0324-3/METRICS, 2017.

de Luca, P., Messori, G., Faranda, D., Ward, P. J., and Coumou, D.: Compound warm-dry and cold-wet events over the Mediterranean, 11, 793–805, https://doi.org/10.5194/ESD-11-793-2020, 2020.

Demiroglu, O. C., Kučerová, J., and Ozcelebi, O.: Snow reliability and climate elasticity: Case of a Slovak ski resort, 70, 1–12, https://doi.org/10.1108/TR-01-2014-0003/FULL/PDF, 2015.

Dzupire, N. C., Ngare, P., and Odongo, L.: A copula based bi-variate model for temperature and rainfall processes, 8, e00365, https://doi.org/10.1016/J.SCIAF.2020.E00365, 2020.

Fisher, R. A. and Tippett, L. H. C.: Limiting forms of the frequency distribution of the largest or smallest member of a sample, 24, 180–190, https://doi.org/10.1017/S0305004100015681, 1928.

Fonseca, D., Carvalho, M. J., Marta-Almeida, M., Melo-Gonçalves, P., and Rocha, A.: Recent trends of extreme temperature indices for the Iberian Peninsula, 94, 66–76, https://doi.org/10.1016/J.PCE.2015.12.005, 2016.

García-Ruiz, J. M., López-Moreno, I. I., Vicente-Serrano, S. M., Lasanta-Martínez, T., and Beguería, S.: Mediterranean water resources in a global change scenario, 105, 121–139, https://doi.org/10.1016/J.EARSCIREV.2011.01.006, 2011.

Gilleland, E. and Katz, R. W.: extRemes 2.0: An Extreme Value Analysis Package in R, 72, 1–39, https://doi.org/10.18637/JSS.V072.I08, 2016.

Gnedenko, B.: Sur La Distribution Limite Du Terme Maximum D'Une Serie Aleatoire, 44, 423, https://doi.org/10.2307/1968974, 1943.

Goda, Y.: Inherent Negative Bias of Quantile Estimates of Annual Maximum Data Due to Sample Size Effect: A Numerical Simulation Study, 53, 397–429, https://doi.org/10.1142/S0578563411002409, 2018.

Goulden, C.: Methods of statistical analysis., 1939.

Hao, Z., Singh, V. P., and Hao, F.: Compound Extremes in Hydroclimatology: A Review, 10, 718, https://doi.org/10.3390/W10060718, 2018.

Hersbach, H., Bell, B., Berrisford, P., Hirahara, S., Horányi, A., Muñoz-Sabater, J., Nicolas, J., Peubey, C., Radu, R., Schepers, D., Simmons, A., Soci, C., Abdalla, S., Abellan, X., Balsamo, G., Bechtold, P., Biavati, G., Bidlot, J., Bonavita, M., de Chiara, G., Dahlgren, P., Dee, D., Diamantakis, M., Dragani, R., Flemming, J., Forbes, R., Fuentes, M., Geer, A., Haimberger, L., Healy, S., Hogan, R. J., Hólm, E., Janisková, M., Keeley, S., Laloyaux, P., Lopez, P., Lupu, C., Radnoti, G., de Rosnay, P., Rozum, I., Vamborg, F., Villaume, S., and Thépaut, J. N.: The ERA5 global reanalysis, 146, 1999–2049, https://doi.org/10.1002/QJ.3803, 2020.

Hochman, A., Marra, F., Messori, G., Pinto, J., Raveh-Rubin, S., Yosef, Y., and Zittis, G.: ESD Reviews: Extreme Weather and Societal Impacts in the Eastern Mediterranean, 1–53, https://doi.org/10.5194/ESD-2021-55, 2021.

Houston, T. G., Changnon, S. A., Ae, T. G. H., and Changnon, S. A.: Freezing rain events: a major weather hazard in the conterminous US, 40, 485–494, https://doi.org/10.1007/S11069-006-9006-0, 2006.

Ionita, M.: The Impact of the East Atlantic/Western Russia Pattern on the Hydroclimatology of Europe from Mid-Winter to Late Spring, Climate 2014, Vol. 2, Pages 296-309, 2, 296–309, https://doi.org/10.3390/CLI2040296, 2014.

James Pickands: Statistical Inference Using Extreme Order Statistics, 3, 119–131, https://doi.org/10.1214/AOS/1176343003, 1975.

Konisky, D. M., Hughes, L., and Kaylor, C. H.: Extreme weather events and climate change concern, 134, 533–547, https://doi.org/10.1007/S10584-015-1555-3/FIGURES/3, 2016.

Kundzewicz, Z. W., Radziejewski, M., and Pińskwar, I.: Precipitation extremes in the changing climate of Europe, 31, 51–58, https://doi.org/10.3354/CR031051, 2006.

Lazoglou, G. and Anagnostopoulou, C.: Joint distribution of temperature and precipitation in the Mediterranean, using the Copula method, 135, 1399–1411, https://doi.org/10.1007/S00704-018-2447-Z/FIGURES/5, 2019.

Lemus-Canovas, M.: Changes in compound monthly precipitation and temperature extremes and their relationship with teleconnection patterns in the Mediterranean, Journal of Hydrology, 608, 127580, https://doi.org/10.1016/J.JHYDROL.2022.127580, 2022.

Leonard, M., Westra, S., Phatak, A., Lambert, M., van den Hurk, B., Mcinnes, K., Risbey, J., Schuster, S., Jakob, D., and Stafford-Smith, M.: A compound event framework for understanding extreme impacts, 5, 113–128, https://doi.org/10.1002/WCC.252, 2014.

Lhotka, O. and Kyselý, J.: Precipitation–temperature relationships over Europe in CORDEX regional climate models, International Journal of Climatology, https://doi.org/10.1002/JOC.7508, 2021.

Llasat, M. C., Turco, M., Quintana-Seguí, P., and Llasat-Botija, M.: The snow storm of 8 March 2010 in Catalonia (Spain): a paradigmatic wet-snow event with a high societal impact, 14, 427–441, https://doi.org/10.5194/NHESS-14-427-2014, 2014.

López-Moreno, J. I., Vicente-Serrano, S. M., Morán-Tejeda, E., Lorenzo-Lacruz, J., Kenawy, A., and Beniston, M.: Effects of the North Atlantic Oscillation (NAO) on combined temperature and precipitation winter modes in the Mediterranean mountains: Observed relationships and projections for the 21st century, Glob Planet Change, 77, 62–76, https://doi.org/10.1016/J.GLOPLACHA.2011.03.003, 2011.

Markantonis, I., Vlachogiannis, D., Sfetsos, T., Kioutsioukis, I., and Politi, N.: An Investigation of cold-wet Compound Events in Greece, https://doi.org/10.5194/EMS2021-188, 2021.

Moalafhi, D. B., Evans, J. P., and Sharma, A.: Evaluating global reanalysis datasets for provision of boundary conditions in regional climate modelling, 47, 2727–2745, https://doi.org/10.1007/S00382-016-2994-X/TABLES/9, 2016.

Moberg, A., Jones, P. D., Lister, D., Walther, A., Brunet, M., Jacobeit, J., Alexander, L. v., Della-Marta, P. M., Luterbacher, J., Yiou, P., Chen, D., Tank, A. M. G. K., Saladié, O., Sigró, J., Aguilar, E., Alexandersson, H., Almarza, C., Auer, I., Barriendos, M., Begert, M., Bergström, H., Böhm, R., Butler, C. J., Caesar, J., Drebs, A., Founda, D., Gerstengarbe, F. W., Micela, G., Maugeri, M., Österle, H., Pandzic, K., Petrakis, M., Srnec, L., Tolasz, R., Tuomenvirta, H., Werner, P. C., Linderholm, H., Philipp, A., Wanner, H., and Xoplaki, E.: Indices for daily temperature and precipitation extremes in Europe analyzed for the period 1901–2000, 111, 22106, https://doi.org/10.1029/2006JD007103, 2006.

Nelsen, R.: An introduction to copulas, 2007.

Pandey, P. K., Das, L., Jhajharia, D., and Pandey, V.: Modelling of interdependence between rainfall and temperature using copula, 4, 867–879, https://doi.org/10.1007/S40808-018-0454-9, 2018.

Pestereva, N. M., Popova, N. Yu., and Shagarov, L. M.: Modern Climate Change and Mountain Skiing Tourism: the Alps and the Caucasus, 1602–1617, 2012.

Politi, N., Nastos, P. T., Sfetsos, A., Vlachogiannis, D., and Dalezios, N. R.: Evaluation of the AWR-WRF model configuration at high resolution over the domain of Greece, 208, 229–245, https://doi.org/10.1016/J.ATMOSRES.2017.10.019, 2018.

Politi, N., Sfetsos, A., Vlachogiannis, D., Nastos, P. T., and Karozis, S.: A Sensitivity Study of High-Resolution Climate Simulations for Greece, 8, 44, https://doi.org/10.3390/CLI8030044, 2020.

Politi, N., Vlachogiannis, D., Sfetsos, A., and Nastos, P. T.: High-resolution dynamical downscaling of ERA-Interim temperature and precipitation using WRF model for Greece, 57, 799–825, https://doi.org/10.1007/S00382-021-05741-9/FIGURES/17, 2021.

Politi, N., Vlachogiannis, D., Sfetsos, A., Nastos, P.T., High resolution projections for extreme temperatures and precipitation over Greece, under review, https://doi.org/10.21203/rs.3.rs-1263740/v1, 2022

Pongrácz, R., Bartholy, J., Gelybó, G., and Szabó, P.: Detected and expected trends of extreme climate indices for the carpathian basin, 15–28, https://doi.org/10.1007/978-1-4020-8876-6_2, 2009.

Raziei, T., Daryabari, J., Bordi, I., Modarres, R., and Pereira, L. S.: Spatial patterns and temporal trends of daily precipitation indices in Iran, 124, 239–253, https://doi.org/10.1007/S10584-014-1096-1/TABLES/1, 2014.

Rockel, B., Will, A., and Hense, A.: The regional climate model COSMO-CLM (CCLM), 17, 347–348, https://doi.org/10.1127/0941-2948/2008/0309, 2008.

Sadegh, M., Moftakhari, H., Gupta, H. v., Ragno, E., Mazdiyasni, O., Sanders, B., Matthew, R., and AghaKouchak, A.: Multihazard Scenarios for Analysis of Compound Extreme Events, 45, 5470–5480, https://doi.org/10.1029/2018GL077317, 2018.

Samuelsson, P., Jones, C. G., Willén, U., Ullerstig, A., Gollvik, S., Hansson, U., Jansson, C., Kjellström, E., Nikulin, G., and Wyser, K.: The Rossby Centre Regional Climate model RCA3: model description and performance, 63, 4–23, https://doi.org/10.1111/J.1600-0870.2010.00478.X, 2016.

Schepsmeier, U., Stoeber, J., Christian, E., and Maintainer, B.: Package "VineCopula" Type Package Title Statistical inference of vine copulas, 2013.

Schwarz, G.: Estimating the Dimension of a Model, https://doi.org/10.1214/aos/1176344136, 6, 461–464, https://doi.org/10.1214/AOS/1176344136, 1978.

Singh, H., Najafi, M. R., and Cannon, A. J.: Characterizing non-stationary compound extreme events in a changing climate based on large-ensemble climate simulations, 56, 1389–1405, https://doi.org/10.1007/S00382-020-05538-2/FIGURES/6, 2021.

Sklar and M.: Fonctions de repartition a n dimensions et leurs marges, 8, 229–231, 1959.

Spiridonov, V., Somot, S., and Déqué, M.: ALADIN-Climate: from the origins to present date, n.d.

Tavakol, A., Rahmani, V., and Harrington, J.: Probability of compound climate extremes in a changing climate: A copula-based study of hot, dry, and windy events in the central United States, 15, 104058, https://doi.org/10.1088/1748-9326/ABB1EF, 2020.

Tošić, I. and Unkašević, M.: Extreme daily precipitation in Belgrade and their links with the prevailing directions of the air trajectories, 111, 97–107, https://doi.org/10.1007/S00704-012-0647-5/FIGURES/9, 2013.

Tringa E and Kostopoulou E: An observational study of the relationships between extreme temperature and precipitation and the surface atmospheric circulation in Greece, n.d.

Trujillo, E., Molotch, N. P., Goulden, M. L., Kelly, A. E., and Bales, R. C.: Elevation-dependent influence of snow accumulation on forest greening, 5, 705–709, https://doi.org/10.1038/ngeo1571, 2012.

Vajda, A., Tuomenvirta, H., Juga, I., Nurmi, P., Jokinen, P., and Rauhala, J.: Severe weather affecting European transport systems: The identification, classification and frequencies of events, 72, 169–188, https://doi.org/10.1007/S11069-013-0895-4/TABLES/3, 2014.

van Meijgaard, E., van Ulft, L. H., van de Berg, W. J., Bosveld, F. C., van den Hurk, B. J. J. M., Lenderink, G., and Siebesma, A. P.: The KNMI regional atmospheric climate model RACMO version 2.1, 2008.

521 Vogel, J., Paton, E., and Aich, V.: Seasonal ecosystem vulnerability to climatic anomalies in the
522 Mediterranean, 18, 5903–5927, https://doi.org/10.5194/BG-18-5903-2021, 2021.

523 Voudouri, A. and Kotta, D.: Factors Determined Snow Accumulation Over the Greater Athens Area
524 During the Latest Snowfall Events, 355–361, https://doi.org/10.1007/978-3-642-29172-2_50, 2013.

525 Wu, X., Hao, Z., Hao, F., and Zhang, X.: Variations of compound precipitation and temperature
526 extremes in China during 1961–2014, Science of The Total Environment, 663, 731–737,
527 https://doi.org/10.1016/J.SCITOTENV.2019.01.366, 2019.

528 Zanocco, C., Boudet, H., Nilson, R., Satein, H., Whitley, H., and Flora, J.: Place, proximity, and
529 perceived harm: extreme weather events and views about climate change, 149, 349–365,
530 https://doi.org/10.1007/S10584-018-2251-X/TABLES/2, 2018.

531 Zhang, W., Luo, M., Gao, S., Chen, W., Hari, V., and Khouakhi, A.: Compound Hydrometeorological
532 Extremes: Drivers, Mechanisms and Methods, 9, 941,
533 https://doi.org/10.3389/FEART.2021.673495/BIBTEX, 2021.

534 Zscheischler, J. and Seneviratne, S. I.: Dependence of drivers affects risks associated with compound
535 events, 3, https://doi.org/10.1126/SCIADV.1700263/SUPPL_FILE/1700263_SM.PDF, 2017.

536 Zscheischler, J., Orth, R., and Seneviratne, S. I.: Bivariate return periods of temperature and
537 precipitation explain a large fraction of European crop yields, 14, 3309–3320,
538 https://doi.org/10.5194/BG-14-3309-2017, 2017.

539 Zscheischler, J., Westra, S., van den Hurk, B. J. J. M., Seneviratne, S. I., Ward, P. J., Pitman, A.,
540 AghaKouchak, A., Bresch, D. N., Leonard, M., Wahl, T., and Zhang, X.: Future climate risk from
541 compound events, 8, 469–477, https://doi.org/10.1038/s41558-018-0156-3, 2018.

542 Zhou, S., Zhang, Y., Williams, A. P., and Gentine, P.: Projected increases in intensity, frequency, and
543 terrestrial carbon costs of compound drought and aridity events, Science Advances, 5,
544 https://doi.org/10.1126/SCIADV.AAU5740/SUPPL_FILE/AAU5740_SM.PDF, 2019.

545 **Code and data availability**

546 Code and results data available upon request.

547 **Author contributions**

551 **Competing interests**

552 The authors declare that they have no conflict of interest.

553

554 **Appendix**

NUMBER	LOCATION	ID	LATITUDE	LONGITUDE	ELEVATION (m)	YEARS
1	Alexandroupoli	16627	40.85	25.917	4	1980-2004
2	Elliniko	16716	37.8877	23.7333	10	1980-2004
3	Ioannina	16642	39.7	20.817	483	1980-2004
4	Irakleio	16754	35.339	25.174	39	1980-2004
5	Kalamata	16726	37.067	22.017	6	1980-2004

6	Kastoria	16614	40.45	21.28	660.95	1980-2004
7	Kerkira	16641	39.603	19.912	1	1980-2004
8	Kithira	16743	36.2833	23.0167	167	1980-2004
9	Larisa	16648	39.65	22.417	73	1980-2004
10	Limnos	16650	39.9167	25.2333	4	1980-2004
11	Methoni	16734	36.8333	21.7	34	1980-2004
12	Milos	16738	36.7167	24.45	183	1980-2004
13	Mitilini	16667	39.059	26.596	4	1980-2004
14	Naxos	16732	37.1	25.383	9	1980-2004
15	Rhodes	16749	36.42896	28.21661	95	1980-2004
16	Samos	16723	37.79368	26.68199	10	1980-2004
17	Skyros	16684	38.9676	24.4872	12	1980-2004
18	Souda	16746	35.4833	24.1167	151	1980-2004
19	Thessaloniki	16622	40.517	22.967	2	1980-2004
20	Tripoli	16710	37.527	22.401	651	1980-2004
21	Zakinthos	16719	37.751	20.887	5	1980-2004
22	Florina	16613	40.78	21.43	619	1980-2002
23	Aktio	16643	38.919	20.772	2	1980-2004
24	Anchialos	16665	39.217	22.8	19	1980-2000
25	Lamia	16675	38.883	22.433	12	1980-2004
26	Andravida	16682	37.92	21.293	10	1980-2004
27	Patras	16689	38.25	21.733	2	1980-1999
28	Tanagra	16699	38.317	23.533	140	1980-2000
29	Chios	16706	38.333	26.133	5	1980-2000
30	Elefsis	16718	38.064	23.556	20	1980-2000

555

556 **Table A1: HNMS stations information.**

557

558

559

560

561